PERGAMON

International Journal of Solids and Structures 36 (1999) 5485–5497

INTERNATIONAL JOURNAL OF SOLIDS and STRUCTURES

www.elsevier.com/locate/ijsolstr

# A high precision element with a central circular hole

A.K. Soh[a,*], Z.F. Long[b]

[a] *Department of Mechanical Engineering, The University of Hong Kong, Pokfulam Road, Hong Kong*
[b] *Beijing Graduate School, China University of Mining and Technology, Beijing, 100083, People's Republic of China*

Received 6 May 1998

**Abstract**

An eight-node rectangular membrane element with a central circular hole has been developed using complex potentials to define stress and strain functions. This new element type can be combined with the conventional elements, e.g., isoparametric elements, with no modifications required. Two numerical examples were employed to illustrate the superiority and versatility of the proposed element type. The results obtained using the said element type are closer to the theoretical results as compared with those obtained by similar types of elements. 

*Keywords:* Complex potentials; Finite elements; Rectangular element; Free boundary; Circular hole

## 1. Introduction

There are many stress problems that require the determination of the stress distributions along the free boundary of a circular hole in a plate subjected to applied loads. The finite element technique has been commonly employed to solve such problems using the conventional elements. However, in order to obtain a reasonably accurate solution of stresses in the vicinity of the hole, which is a stress concentration region, a large number of elements are required to model this region. The problem is aggravated if one attempts to determine the stress distributions along the free boundary of the hole with high degree of accuracy (Soh, 1992). This weakness of the conventional finite element technique is due to the fact that, in general, the chosen element displacement functions do not implicitly satisfy the conditions that prevail at a free boundary. As a result, calculations of the boundary stresses based on the element nodal displacements yield non-zero values for the shear and normal stress components, with a corresponding error in the tangential stresses. Soh (1998) has proposed special finite elements to eliminate the said weakness of the conventional finite element technique. However, the number of elements required to model the region surrounding the hole cannot be reduced with the employment of the special elements. Soh

* Corresponding author. Fax: 852 2858 5415; e-mail: aksoh@hkucc.hku.hk

0020-7683/99/$ - see front matter 
PII: S0020-7683(98)00247-9

and Long (1998) have proposed two new element types, one is an eight-node rectangular element with a central circular hole and the other is an eight-node circular element also with a hole, to eliminate the above-mentioned weakness using only one element for the region surrounding the hole. However, the accuracy of these two element types can be further enhanced by careful selection of the complex potentials employed to define the stress and strain functions in the element.

In this paper, a new element type will be developed using complex potentials. Two numerical examples will be employed to illustrate the superiority and versatility of the proposed element type, which can be used together with the conventional elements, e.g., isoparametric elements, with no modifications required.

## 2. Analysis

For a two-dimensional plate with a circular hole, as shown in Fig. 1, the stress ($\sigma$) and displacement ($u$) fields are most effectively expressed in terms of the complex potentials of Muskhelishvili (1954) as follows:

$$\sigma_{xx}+\sigma_{yy} = 2\{\psi'(z)+\overline{\psi'(z)}\} \tag{1}$$

$$\sigma_{yy}-\sigma_{xx}+2i\tau_{xy} = 2\{\bar{z}\psi''(z)+\chi'(z)\} \tag{2}$$

$$2\mu(u_x+iu_y) = \kappa\psi(z)-z\overline{\psi'(z)}-\overline{\chi(z)} \tag{3}$$

$$\begin{aligned} F_x+iF_y &= -i[\psi(z)+z\overline{\psi'(z)}+\overline{\chi(z)}]_{\mathrm{A}}^{\mathrm{B}} \\ &= -i[\psi(z_{\mathrm{B}})+z_{\mathrm{B}}\overline{\psi'(z_{\mathrm{B}})}+\overline{\chi(z_{\mathrm{B}})}-C_{\mathrm{A}}] \end{aligned} \tag{4}$$

where $z = x+iy$, $\psi(z)$ and $\chi(z)$ are holomorphic functions, $\psi'(z) = \mathrm{d}\psi(z)/\mathrm{d}z$, and the overbar denotes complex conjugate; $\kappa = 3-4v$ for plane strain and $(3-v)/(1+v)$ for plane stress; $\mu$ and $v$ are the shear modulus and Poisson's ratio, respectively, of the material; $F_x$ and $F_y$ are the $x$- and

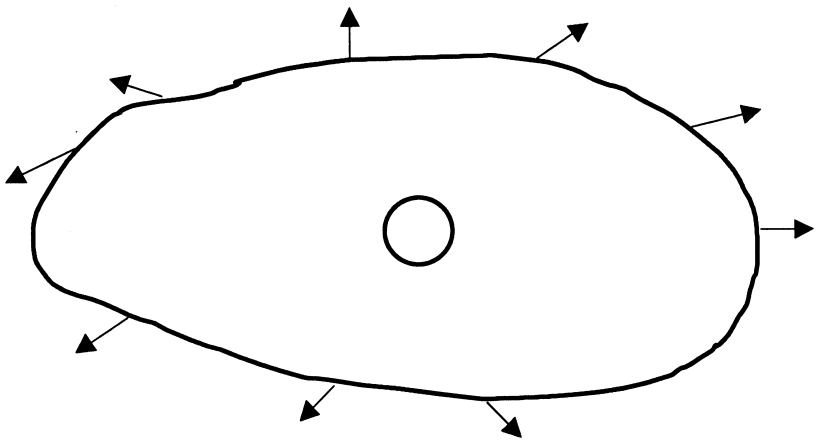

Fig. 1. A two-dimensional plate with a circular hole subjected to prescribed loads.

$y$-components of the resultant force acting on the boundary of the circular hole from point A to B; and $C_A$ is a complex constant at the datum point A.

Equations (1) and (2) can be expressed in terms of polar coordinates $r$ and $\theta$ as follows:

$$\sigma_r+\sigma_\theta = 2\{\psi'(z)+\overline{\psi'(z)}\} \tag{5}$$

$$\sigma_\theta-\sigma_r+2i\tau_{r\theta} = 2\,e^{2i\theta}\{\bar{z}\psi''(z)+\chi'(z)\} \tag{6}$$

From eqns (5) and (6), we obtain

$$\sigma_r-i\tau_{r\theta} = \psi'(z)+\overline{\psi'(z)}-e^{2i\theta}\{\bar{z}\psi''(z)+\chi'(z)\} \tag{7}$$

The conditions to be satisfied at the free boundary of the circular hole in a plate are

$$\sigma_r = \tau_{r\theta} = 0 \tag{8}$$

Therefore,

$$\psi'(z_0)+\overline{\psi'(z_0)}-e^{2i\theta}\{\bar{z}_0\psi''(z_0)+\chi'(z_0)\} = 0 \tag{9}$$

where $z_0 = a\,e^{i\theta}$ and $a$ is the radius of the circular hole.

The two holomorphic functions $\psi(z)$ and $\chi(z)$ can be represented by the Laurent series of $z$ as follows:

$$\begin{aligned}\psi(z) &= \psi^0+\sum_{j=1}^{j_l}A_jz^j+\sum_{k=1}^{k_l}B_kz^{-k}\\ \chi(z) &= \chi^0+\sum_{m=1}^{m_l}C_mz^m+\sum_{n=1}^{n_l}D_nz^{-n}\end{aligned}\qquad \text{where } \|z\|\geqslant a \tag{10}$$

where $j_l$, $k_l$, $m_l$ and $n_l$ are the upper limits of the series; $A_j$, $B_k$, $C_m$ and $D_n$ are complex coefficients with the forms $A_j = \hat{A}_j+i\tilde{A}_j$, $B_k = \hat{B}_k+i\tilde{B}_k$, $C_m = \hat{C}_m+i\tilde{C}_m$ and $D_n = \hat{D}_n+i\tilde{D}_n$; and $\hat{A}_j$, $\tilde{A}_j$, $\hat{B}_k$, $\tilde{B}_k$, $\hat{C}_m$, $\tilde{C}_m$, $\hat{D}_n$, $\tilde{D}_n$ are real numbers.

The terms $\psi^0$ and $\chi^0$ are rigid body translations which can be related by implementing the conditions that $F_x = F_y = 0$ at the free boundary of the hole, i.e.,

$$\psi(z_0)+z_0\overline{\psi'(z_0)}+\overline{\chi(z_0)}-C_A = 0 \tag{11}$$

Therefore, $\psi^0+\overline{\chi^0} = 0$. Thus, eqn (10) can be re-written as

$$\begin{aligned}\psi(z) &= \alpha_0+\sum_{j=1}^{j_l}A_jz^j+\sum_{k=1}^{k_l}B_kz^{-k}\\ \chi(z) &= -\bar{\alpha}_0+\sum_{m=1}^{m_l}C_mz^m+\sum_{n=1}^{n_l}D_nz^{-n}\end{aligned}\qquad \text{where } \|z\|\geqslant a \tag{12}$$

### 2.1. Formulation of an eight-node rectangular element with a central circular hole

An eight-node rectangular membrane element with a circular hole is shown in Fig. 2. The nodal displacements vector, $\{\boldsymbol{\delta}\}^e$, is defined as

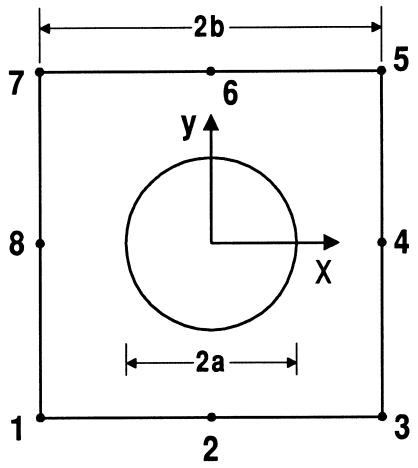


Fig. 2. An eight-node rectangular element with a circular hole.

$$\{\boldsymbol{\delta}\}^{\mathrm{e}} = \{(u_x)_1,(u_y)_1,(u_x)_2,(u_y)_2,\ldots,(u_x)_8,(u_y)_8\}^{\mathrm{T}} \tag{13}$$

where $(u_x)_i$ and $(u_y)_i$ denote the $x$- and $y$-displacement components of node $i$, respectively.

In order to express $\psi(z)$ and $\chi(z)$ in terms of $\{\boldsymbol{\delta}\}^{\mathrm{e}}$, the number of terms employed to define these functions, as given by eqn (12), were chosen to be $j_l = 4$, $k_l = m_l = 3$ and $n_l = 5$. Substituting eqn (12) into eqn (9), the following equations were obtained,

$$\left.\begin{aligned}
&\hat{D}_1 = -2a^2\hat{A}_1, \quad \tilde{D}_1 = 0\\
&D_2 = -a^4\bar{A}_2\\
&3A_3a^4 + \bar{B}_1 + a^2C_1 = 0\\
&\bar{A}_3a^4 - B_1 + a^{-2}D_3 = 0\\
&4A_4a^6 + \bar{B}_2 + a^4C_2 = 0\\
&\bar{A}_4a^6 - 2B_2 + a^{-2}D_4 = 0\\
&\bar{B}_3 + a^6C_3 = 0\\
&-3B_3 + a^{-2}D_5 = 0
\end{aligned}\right\} \tag{14}$$

Substituting eqn (14) into eqn (12), we obtain

$$\psi(z) = \alpha_0 + \sum_{j=1}^{4} A_jz^j + [(a^4\hat{A}_3 + a^{-2}\hat{D}_3) + i(-a^4\tilde{A}_3 + a^{-2}\tilde{D}_3)]z^{-1}$$

$$+ \frac{1}{2}[(a^6\hat{A}_4 + a^{-2}\hat{D}_4) + i(-a^6\tilde{A}_4 + a^{-2}\tilde{D}_4)]z^{-2} + \frac{1}{3}a^{-2}(\hat{D}_5 + i\tilde{D}_5)z^{-3} \tag{15a}$$

$$\chi(z) = -\bar{\alpha}_0 + [-(4a^2\hat{A}_3 + a^{-4}\hat{D}_3) + i(-4a^2\tilde{A}_3 + a^{-4}\tilde{D}_3)]z$$
$$+\tfrac{1}{2}[-(9a^2\hat{A}_4 + a^{-6}\hat{D}_4) + i(-9a^2\tilde{A}_4 + a^{-6}\tilde{D}_4)]z^2$$
$$-\tfrac{1}{3}a^{-8}(\hat{D}_5 - i\tilde{D}_5)z^3 - 2a^2\hat{A}_1 z^{-1} - a^4(\hat{A}_2 - i\tilde{A}_2)z^{-2} + D_3 z^{-3} + D_4 z^{-4} + D_5 z^{-5} \quad (15b)$$

Substituting eqns (15) into eqn (3), the displacement field in the element can be expressed in terms of the independent coefficients as follows:

$$\{\boldsymbol{\delta}\} = \begin{Bmatrix} u_x \\ u_y \end{Bmatrix} = \frac{1}{2\mu}[\boldsymbol{\Omega}]\{\boldsymbol{\Gamma}\} \quad (16)$$

where

$$[\boldsymbol{\Omega}] = \begin{bmatrix} \boldsymbol{\Omega}_x \\ \boldsymbol{\Omega}_y \end{bmatrix}$$

and

$$\{\boldsymbol{\Gamma}\} = \{\hat{\alpha}_0, \tilde{\alpha}_0, \hat{A}_1, \tilde{A}_1, \hat{A}_2, \tilde{A}_2, \hat{A}_3, \tilde{A}_3, \hat{D}_3, \tilde{D}_3, \hat{A}_4, \tilde{A}_4, \hat{D}_4, \tilde{D}_4, \hat{D}_5, \tilde{D}_5\}^{\mathrm{T}}$$

The two sub-matrices, $[\boldsymbol{\Omega}_x]$ and $\lfloor \boldsymbol{\Omega}_y \rfloor$ are given by

$$[\boldsymbol{\Omega}_x]^{\mathrm{T}} = \begin{bmatrix}
\kappa + 1 \\
0 \\
\kappa r\cos\theta - r\cos\theta + (2a^2/r)\cos\theta \\
-\kappa r\sin\theta - r\sin\theta \\
\kappa r^2\cos 2\theta - 2r^2 + a^4 r^{-2}\cos 2\theta \\
-\kappa r^2\sin 2\theta - a^4 r^{-2}\sin 2\theta \\
\kappa r^3\cos 3\theta - 3r^3\cos\theta + (a^4\kappa/r)\cos\theta + (a^4/r)\cos 3\theta + 4a^2 r\cos\theta \\
-\kappa r^3\sin 3\theta + 3r^3\sin\theta - (a^4\kappa/r)\sin\theta - (a^4/r)\sin 3\theta - 4a^2 r\sin\theta \\
\kappa a^{-2}r^{-1}\cos\theta + a^{-2}r^{-1}\cos 3\theta + a^{-4}r\cos\theta - r^{-3}\cos 3\theta \\
\kappa a^{-2}r^{-1}\sin\theta + a^{-2}r^{-1}\sin 3\theta + a^{-4}r\sin\theta - r^{-3}\sin 3\theta \\
\kappa r^4\cos 4\theta + (\kappa a^6 r^{-2}/2)\cos 2\theta - 4r^4\cos 2\theta + a^6 r^{-2}\cos 4\theta + (9a^2r^2/2)\cos 2\theta \\
-\kappa r^4\sin 4\theta - (\kappa a^6 r^{-2}/2)\sin 2\theta + 4r^4\sin 2\theta - a^6 r^{-2}\sin 4\theta - (9a^2r^2/2)\sin 2\theta \\
(\kappa a^{-2}r^{-2}/2)\cos 2\theta + a^{-2}r^{-2}\cos 4\theta + (a^{-6}r^2/2)\cos 2\theta - r^{-4}\cos 4\theta \\
(\kappa a^{-2}r^{-2}/2)\sin 2\theta + a^{-2}r^{-2}\sin 4\theta + (a^{-6}r^2/2)\sin 2\theta - r^{-4}\sin 4\theta \\
(\kappa a^{-2}r^{-3}/3)\cos 3\theta + a^{-2}r^{-3}\cos 5\theta + (a^{-8}r^3/3)\cos 3\theta - r^{-5}\cos 5\theta \\
(\kappa a^{-2}r^{-3}/3)\sin 3\theta + a^{-2}r^{-3}\sin 5\theta + (a^{-8}r^3/3)\sin 3\theta - r^{-5}\sin 5\theta
\end{bmatrix}$$

$$[\boldsymbol{\Omega}_y]^{\mathrm{T}} = \begin{bmatrix} 0 \\ \kappa+1 \\ \kappa r\sin\theta - r\sin\theta + (2a^2/r)\sin\theta \\ \kappa r\cos\theta + r\cos\theta \\ \kappa r^2\sin 2\theta + a^4 r^{-2}\sin 2\theta \\ \kappa r^2\cos 2\theta + 2r^2 + a^4 r^{-2}\cos 2\theta \\ \kappa r^3\sin 3\theta + 3r^3\sin\theta - (a^4\kappa/r)\sin\theta + (a^4/r)\sin 3\theta - 4a^2 r\sin\theta \\ \kappa r^3\cos 3\theta + 3r^3\cos\theta - (a^4\kappa/r)\cos\theta + (a^4/r)\cos 3\theta - 4a^2 r\cos\theta \\ -\kappa a^{-2}r^{-1}\sin\theta + a^{-2}r^{-1}\sin 3\theta - a^{-4}r\sin\theta - r^{-3}\sin 3\theta \\ \kappa a^{-2}r^{-1}\cos\theta - a^{-2}r^{-1}\cos 3\theta + a^{-4}r\cos\theta + r^{-3}\cos 3\theta \\ \kappa r^4\sin 4\theta - (\kappa a^6 r^{-2}/2)\sin 2\theta + 4r^4\sin 2\theta + a^6 r^{-2}\sin 4\theta - (9a^2r^2/2)\sin 2\theta \\ \kappa r^4\cos 4\theta - (\kappa a^6 r^{-2}/2)\cos 2\theta + 4r^4\cos 2\theta + a^6 r^{-2}\cos 4\theta - (9a^2r^2/2)\cos 2\theta \\ -(\kappa a^{-2}r^{-2}/2)\sin 2\theta + a^{-2}r^{-2}\sin 4\theta - (a^{-6}r^2/2)\sin 2\theta - r^{-4}\sin 4\theta \\ (\kappa a^{-2}r^{-2}/2)\cos 2\theta - a^{-2}r^{-2}\cos 4\theta + (a^{-6}r^2/2)\cos 2\theta + r^{-4}\cos 4\theta \\ -(\kappa a^{-2}r^{-3}/3)\sin 3\theta + a^{-2}r^{-3}\sin 5\theta - (a^{-8}r^3/3)\sin 3\theta - r^{-5}\sin 5\theta \\ (\kappa a^{-2}r^{-3}/3)\cos 3\theta - a^{-2}r^{-3}\cos 5\theta + (a^{-8}r^3/3)\cos 3\theta + r^{-5}\cos 5\theta \end{bmatrix}$$

Substituting the nodal displacements at the eight-nodal points of the element into eqn (16), we obtain

$$2\mu\{\boldsymbol{\delta}\}^{\mathrm{e}} = \begin{bmatrix} (\boldsymbol{\Omega}_x)_1 \\ (\boldsymbol{\Omega}_y)_1 \\ \vdots \\ (\boldsymbol{\Omega}_x)_8 \\ (\boldsymbol{\Omega}_y)_8 \end{bmatrix} \{\boldsymbol{\Gamma}\} = [\boldsymbol{\Lambda}]\{\boldsymbol{\Gamma}\} \tag{17}$$

where $\{\boldsymbol{\Lambda}\}$ is a coefficient matrix consisting of products $r$ and $\theta$.

Equation (17) can be expressed as

$$\{\boldsymbol{\Gamma}\} = 2\mu[\boldsymbol{\Lambda}]^{-1}\{\boldsymbol{\delta}\}^{\mathrm{e}} \tag{18}$$

Note that the inverse of $[\boldsymbol{\Lambda}]$ may not exist occasionally when the choice of $j_l$, $k_l$, $m_l$ and $n_l$ in eqn (10) is varied.

Substituting eqn (18) into eqn (16), we obtain

$$\{\boldsymbol{\delta}\} = [\boldsymbol{\Omega}][\boldsymbol{\Lambda}]^{-1}\{\boldsymbol{\delta}\}^{\mathrm{e}} = [\boldsymbol{N}]\{\boldsymbol{\delta}\}^{\mathrm{e}} \tag{19}$$

where $[\boldsymbol{N}] = [\boldsymbol{\Omega}][\boldsymbol{\Lambda}]^{-1}$ is termed as the element shape function by analogy with the traditional finite element method.

By adopting the standard finite element approach, we obtain

$$\{\boldsymbol{\varepsilon}\} = \begin{bmatrix} \partial u_x/\partial x \\ \partial u_y/\partial y \\ \partial u_x/\partial y + \partial u_y/\partial x \end{bmatrix} = \begin{bmatrix} \partial \boldsymbol{\Omega}_x/\partial x \\ \partial \boldsymbol{\Omega}_y/\partial y \\ \partial \boldsymbol{\Omega}_x/\partial y + \partial \boldsymbol{\Omega}_y/\partial x \end{bmatrix} [\boldsymbol{\Lambda}]^{-1} \{\boldsymbol{\delta}\}^{\mathrm{e}} = [\boldsymbol{B}]\{\boldsymbol{\delta}\}^{\mathrm{e}}$$

where $[\boldsymbol{B}]$ is the element strain displacement matrix.

The element stiffness matrix is given by

$$[\boldsymbol{K}]^{\mathrm{e}} = \int_{\mathrm{vol}} [\boldsymbol{B}]^{\mathrm{T}} [\boldsymbol{D}][\boldsymbol{B}] \, \mathrm{d(vol)} \tag{20}$$

where $[\boldsymbol{D}]$ is the element elasticity matrix. This element is called WCH-R8-2.

Note that $[\boldsymbol{K}]^{\mathrm{e}}$ is evaluated by first dividing the domain of the element, excluding the central hole, into $N \times N$ subdomains, where $N$ is a chosen integer. The integration is then carried out by summing the products of the centroidal value of $[\boldsymbol{B}]^{\mathrm{T}}[\boldsymbol{D}][\boldsymbol{B}]$ and $d(\mathrm{vol})$ for the $N \times N$ subdomains.

Once all the nodal displacements are determined, the nodal and boundary stresses of the element can be easily calculated by employing the strain–displacement equations and stress–strain relations.

## 3. Numerical examples

### 3.1. Thick-walled cylinder subjected to uniform pressure

Consider a thick-walled cylinder subjected to uniform pressure on the outer surface, as shown in Fig. 3(a). A finite element model, which consists of 1 eight-node rectangular element with a circular hole and 20 eight-node isoparametric elements, as shown in Fig. 3(b), was devised for analyzing the said problem. Five analyses were performed using the model devised, by varying the ratio of the diameter of the hole to the side length of the proposed rectangular element. The normalized hoop stresses, $-\sigma_\theta/p$, obtained along the free boundary of the circular hole are presented in Table 1. It is obvious that the results obtained using the proposed element are in extremely good agreement with the theoretical results (Xu, 1992). Moreover, the discrepancies between these two sets of results are smaller as compared with the corresponding discrepancies between the theoretical results and those obtained by Soh and Long (1998) using a similar rectangular element, called WCH-R8-1.

### 3.2. Square plate with a circular hole subjected to prescribed loads

Figures 4(a) and (b) show a square plate with a small central circular hole subjected to two different load cases. The domain of the square plate with a circular hole is discretized into 25 elements, for which one is the proposed element and the rest are eight-node isoparametric elements, as shown in Fig. 5. Similar to the first example, five analyses were performed using the model devised for each of the load cases considered. These five analyses were carried out by varying the ratio of the diameter of the hole to the side length of the proposed rectangular element. The normalized hoop stresses, $\sigma_\theta/\sigma_0$, obtained along the free boundary of the circular hole are presented in Table 2 for the load case in which the plate is subjected to uniform tensile stress, $\sigma_0$, in both the

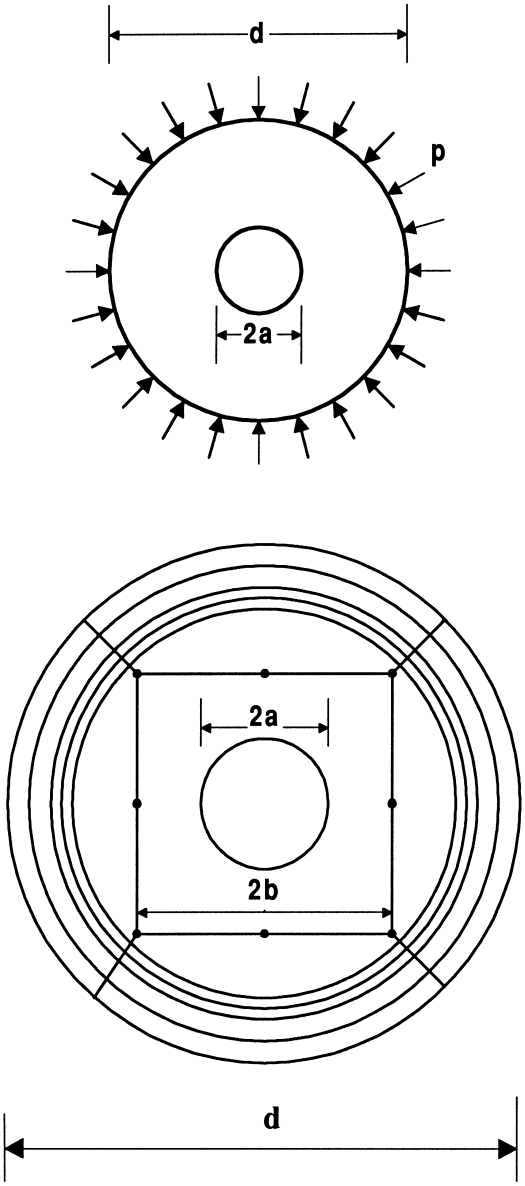


Fig. 3. (a) A thick-walled cylinder subjected to uniform pressure on the outer surface. (b) One eight-node rectangular element with a circular hole and 20 eight-node isoparametric elements.

$x$- and $y$-directions. The corresponding stresses are presented in Table 3 for the load case in which the plate is subjected to uniform tensile stress, $\sigma_0$, in the $x$-direction.

In both load cases (refer to Tables 2 and 3), the results obtained using the proposed rectangular element, i.e., WCH-R8-2, are again superior to those obtained by Soh and Long (1998) using a similar rectangular element, i.e., WCH-R8-1, as compared with the theoretical results (Xu, 1992).

Table 1
Normalized stress ($-\sigma_\theta/p$) at the bore of a thick-walled cylinder subjected to a uniform pressure on the outer surface

| | Normalized stress $-\sigma_\theta/p$ | | | | | | | | | |
|---|---|---|---|---|---|---|---|---|---|---|
| $a/b$* | 0.5 | | 0.4 | | 0.3 | | 0.2 | | 0.1 | |
| $2a/d$† | 0.25 | | 0.20 | | 0.15 | | 0.10 | | 0.05 | |
| $\theta$ (°) | WCH-R8-1 | WCH-R8-2 | WCH-R8-1 | WCH-R8-2 | WCH-R8-1 | WCH-R8-2 | WCH-R8-1 | WCH-R8-2 | WCH-R8-1 | WCH-R8-2 |
| 0 | 2.1997 | 2.1712 | 2.1219 | 2.1099 | 2.0671 | 2.0609 | 2.0282 | 2.0254 | 2.0072 | 2.0066 |
| 15 | 2.1927 | 2.1684 | 2.1195 | 2.1071 | 2.0664 | 2.0598 | 2.0281 | 2.0251 | 2.0072 | 2.0066 |
| 30 | 2.1788 | 2.1629 | 2.1147 | 2.1015 | 2.0650 | 2.0574 | 2.0278 | 2.0246 | 2.0072 | 2.0066 |
| 45 | 2.1718 | 2.1601 | 2.1122 | 2.0987 | 2.0664 | 2.0562 | 2.0277 | 2.0243 | 2.0072 | 2.0065 |
| 60 | 2.1788 | 2.1629 | 2.1147 | 2.1015 | 2.0650 | 2.0574 | 2.0278 | 2.0246 | 2.0072 | 2.0066 |
| 75 | 2.1927 | 2.1684 | 2.1195 | 2.1071 | 2.0664 | 2.0598 | 2.0281 | 2.0251 | 2.0072 | 2.0066 |
| 90 | 2.1997 | 2.1712 | 2.1219 | 2.1099 | 2.0671 | 2.0609 | 2.0282 | 2.0254 | 2.0072 | 2.0066 |
| Theoretical solution | 2.1333 | | 2.0833 | | 2.0460 | | 2.0202 | | 2.0050 | |

* $a$ = the radius of the circular hole; $b$ = half the side length of WCH-R8-1 and WCH-R8-2 elements.
† $d$ = the outer diameter of the thick-walled cylinder.

The only exception occurs in the second load case at $\theta = 0^\circ$ for $a/b = 0.4$ and 0.5, in which the reverse is true. However, it is a fair claim that the results obtained by the proposed element are in extremely good agreement with the theoretical results for both load cases, and the proposed element is superior to WCH-R8-1.

## 4. Conclusions

A high precision eight-node rectangular element with a central circular hole has been developed. The superiority and versatility of the proposed element type has been illustrated using two numerical examples. The results obtained by this element type are in extremely good agreement with the theoretical solutions and superior to the corresponding results obtained by Soh and Long (1998) using similar types of elements. The improvement in accuracy achieved by the proposed element type is due to careful selection of the complex potentials employed to define the stress and strain functions in the element. Note that although the proposed element is a rectangular element, it can be used together with the conventional elements, e.g., isoparametric elements, to calculate stresses around a hole which has its centre away from that of the structure analysed. Moreover, the proposed element can be made non-rectangular by making slight modification to the element formulation.

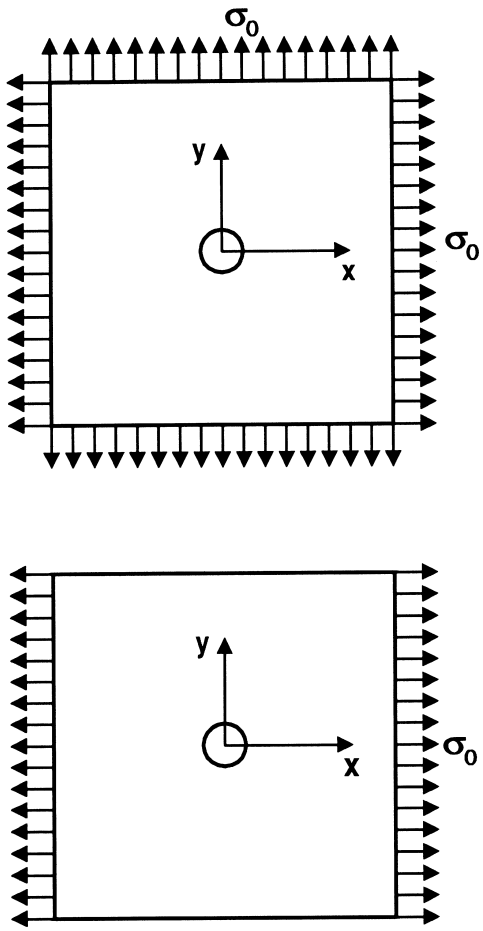


Fig. 4. (a) A square plate with a small central circular hole subjected to tensile stress in the $x$- and $y$-directions. (b) A square plate with a small central circular hole subjected to tensile stress in the $x$-direction.

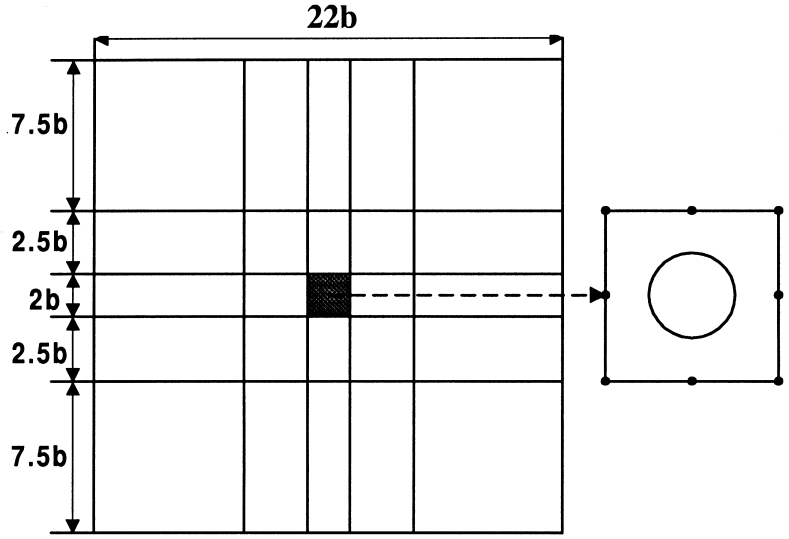


Fig. 5. Mesh of the square plate with a small central circular hole.

Table 2
Normalized stresses, $\sigma_\theta/\sigma_0$, at the hole in a square plate subjected to uniform tensile stress in the $x$- and $y$-directions

| | Normalized stress $\sigma_\theta/\sigma_0$ | | | | | | | | | |
|---|---|---|---|---|---|---|---|---|---|---|
| $a/b$* | 0.5 | | 0.4 | | 0.3 | | 0.2 | | 0.1 | |
| ($w$† = 22$b$) $\theta$ (°) | WCH-R8-1 | WCH-R8-2 | WCH-R8-1 | WCH-R8-2 | WCH-R8-1 | WCH-R8-2 | WCH-R8-1 | WCH-R8-2 | WCH-R8-1 | WCH-R8-2 |
| 0 | 1.9779 | 2.0106 | 1.9665 | 2.0070 | 1.9594 | 2.0037 | 1.9532 | 2.0006 | 1.9507 | 2.0004 |
| 15 | 1.9726 | 2.0067 | 1.9645 | 2.0045 | 1.9588 | 2.0027 | 1.9531 | 2.0004 | 1.9507 | 2.0004 |
| 30 | 1.9619 | 1.9988 | 1.9606 | 1.9996 | 1.9575 | 2.0008 | 1.9528 | 1.9999 | 1.9506 | 2.0003 |
| 45 | 1.9561 | 1.9945 | 1.9584 | 1.9969 | 1.9567 | 1.9997 | 1.9525 | 1.9996 | 1.9506 | 2.0003 |
| 60 | 1.9607 | 1.9979 | 1.9598 | 1.9989 | 1.9570 | 2.0004 | 1.9525 | 1.9997 | 1.9506 | 2.0003 |
| 75 | 1.9705 | 2.0051 | 1.9631 | 2.0034 | 1.9579 | 2.0020 | 1.9527 | 2.0000 | 1.9507 | 2.0003 |
| 90 | 1.9754 | 2.0085 | 1.9648 | 2.0055 | 1.9585 | 2.0028 | 1.9529 | 2.0002 | 1.9508 | 2.0003 |
| Theoretical solution | 2.0000 | | | | | | | | | |

* $a$ = the radius of the circular hole; $b$ = half the side length of WCH-R8-1 and WCH-R8-2 elements.
† $w$ = plate width.

Table 3
Normalized stresses, $\sigma_\theta/\sigma_0$, at the hole in a square plate subjected to uniform tensile stress in the $x$-direction

| | | Normalized stress $\sigma_\theta/\sigma_0$ (% discrepancy) | | | |
|---|---|---|---|---|---|
| $\theta$ (°) | | 0 | 45 | 60 | 90 |
| $a/b^* = 0.5$ ($w\dagger = 22b$) | WCH-R8-1 | −0.9872 (1.3) | 0.9783 (−2.2) | 1.9683 (−1.6) | 2.9620 (−1.3) |
| | WCH-R8-2 | −0.9708 (−2.9) | 0.9974 (−0.3) | 1.9868 (−0.7) | 2.9786 (−0.7) |
| $a/b^* = 0.4$ ($w\dagger = 22b$) | WCH-R8-1 | −1.0060 (0.6) | 0.9793 (−2.1) | 1.9743 (−1.3) | 2.9704 (−1.0) |
| | WCH-R8-2 | −0.9857 (−1.4) | 0.9985 (−0.2) | 1.9938 (−0.3) | 2.9908 (−0.3) |
| $a/b^* = 0.3$ ($w\dagger = 22b$) | WCH-R8-1 | −1.0213 (2.10) | 0.9784 (−2.2) | 1.9789 (−1.1) | 2.9796 (−0.7) |
| | WCH-R8-2 | −0.9992 (−0.1) | 0.9998 (0.0) | 2.0005 (0.0) | 3.0018 (0.1) |
| $a/b^* = 0.2$ ($w\dagger = 22b$) | WCH-R8-1 | −1.0267 (2.7) | 0.9762 (−2.4) | 1.9778 (−1.1) | 2.9795 (−0.7) |
| | WCH-R8-2 | −1.0030 (0.3) | 0.9998 (0.0) | 2.0014 (0.1) | 3.0031 (0.1) |
| $a/b^* = 0.1$ ($w\dagger = 22b$) | WCH-R8-1 | −1.0277 (2.8) | 0.9753 (−2.5) | 1.9768 (−1.2) | 2.9784 (−0.7) |
| | WCH-R8-2 | −1.0028 (0.3) | 1.0001 (0.0) | 2.0016 (0.1) | 3.0031 (0.1) |
| Theoretical solution | | −1.0 | 1.0 | 2.0 | 3.0 |

* $a$ = the radius of the circular hole; $b$ = half the side length of WCH-R8-1 and WCH-R8-2 elements.
† $w$ = plate width.

## Acknowledgment

This study was supported by the CRCG-fund of the University of Hong Kong.

## References

Muskhelishvili, N., 1954. Stress function. Complex representation of the general solution of the equations of the plane theory of elasticity. Some Basic Problems of the Mathematical Theory of Elasticity, 2nd Ed. Noordhoof International Publishing, Netherlands, pp. 105–166.

Soh, A.K., 1992. An improved method for determining free boundary stresses. Journal of Strain Analysis 27(2), pp. 93–99.

Soh, A.K., 1998. Development of special finite elements for free boundaries. International Journal of Solids and Structures, accepted.

Soh, A.K., Long, Z.F., 1998. Development of membrane elements with a central circular hole. International Journal for Numerical Methods in Engineering, submitted.

Xu, Z.L., 1992. Solution of plane problems in polar coordinates. Applied Elasticity, English edition. Wiley Eastern Limited, New Delhi, pp. 54–83.